
Intraocular lens tilt and decentration
measurements:

Purkinje imaging versus
Scheimpflug imaging

5

*5 IOL tilt and decentration measurements:
Purkinje imaging versus Scheimpflug
imaging*

This chapter is based on the article by de Castro. A et al., “*Tilt and decentration of intraocular lenses in vivo from Purkinje and Scheimpflug imaging: a validation study*” J. Cataract Refractive Surg. Vol 33, 418-429. Coauthors of the study are S.Marcos and P.Rosales. The contribution of Patricia Rosales to the study was data acquisition and processing of Purkinje images on the artificial eye, on normal subjects and on patients with IOLs.

RESUMEN

Objetivos: Se presenta una comparación de medidas de inclinación y descentramiento de la lente, obtenidas a partir de imágenes de Scheimpflug tomadas con una cámara de Scheimpflug comercial (Pentacam, Oculus) e imágenes de Purkinje.

Métodos: Las medidas de inclinación y descentramiento de la lente se realizaron empleando una cámara de Scheimpflug comercial (Pentacam, Oculus), con algoritmos propios para calcular la inclinación y el descentramiento de la lente y un sistema de imágenes de Purkinje desarrollado en el laboratorio. Las medidas se realizaron sobre un ojo artificial, y en veinte y un ojos de 12 pacientes operados de cirugía de cataratas.

Resultados: Las medidas realizadas sobre el ojo artificial, presentaban una discrepancia en valor absoluto, respecto del valor nominal de 0.279 deg (Purkinje) y 0.243 deg (Scheimpflug) para medidas de inclinación, y 0.0094 mm (Purkinje) y 0.228 mm (Scheimpflug) para descentramiento. En medidas realizadas sobre pacientes con lentes intraoculares implantadas se encontró una inclinación promedio menor que 2.6 deg y un valor de descentramiento promedio menor que 0.4 mm. Se observa una simetría entre ojos derecho e izquierdo para inclinación y descentramiento horizontal, tanto empleando ambos métodos.

Conclusiones: Ambos sistemas muestran una alta reproducibilidad. Las medidas realizadas sobre el ojo artificial muestran una mayor precisión empleando el sistema de imágenes de Purkinje que los algoritmos aplicados a las imágenes de Scheimpflug. Las medidas de inclinación y descentramiento en dirección horizontal están muy correlacionadas. Las medidas muestran que las lentes intraoculares tienden a estar inclinadas y descentradas nasalmente en la mayoría de los pacientes.

ABSTRACT

Purpose: To measure tilt and decentration of intraocular lenses (IOLs) with Scheimpflug and Purkinje imaging systems.

Methods: Measurements of IOL tilt and decentration were obtained using a commercial Scheimpflug system (Pentacam, Oculus) and custom algorithms, and a custom-built Purkinje imaging apparatus. Both methods were validated with a physical model eye where tilt and decentration can be set nominally. Twenty-one eyes of 12 patients with IOL implanted were measured with both systems.

Results: Slopes and correlation coefficients of measurements on the physical model eye showed an absolute discrepancy between nominal and measured values of 0.279 deg (Purkinje) and 0.243 deg (Scheimpflug) for tilt and 0.094 mm (Purkinje) and 0.228 mm (Scheimpflug) for decentration. In patients, we found an average tilt less than 2.6 deg and average decentration less than 0.4 mm. We found mirror symmetry between right and left eyes for tilt around vertical axis and for decentration in the horizontal axis, as revealed by both techniques.

Conclusions: Both systems show a high reproducibility. Validation experiments on physical model eyes shows slightly higher accuracy with the Purkinje than the Scheimpflug imaging method. Horizontal measurements on patients from both techniques are highly correlated. IOLs tend to be tilted and decentered nasally in most patients.

1. INTRODUCTION

Although some studies reporting measurements of IOL tilt and decentration in vivo with Purkinje imaging and Scheimpflug imaging have been published, to our knowledge no validation studies of these techniques have been presented. The Purkinje imaging system developed in this thesis to measure tilt and decentration of the crystalline lens has been described in detail in Chapter 2. In research projects undergoing at the Visual Optics and Biophotonics lab, routines to measure tilt and decentration from Scheimpflug imaging have been developed in parallel by Alberto de Castro (de Castro, Rosales & Marcos, 2007). The Scheimpflug camera provides images of the anterior chamber of the eye. Its configuration is such that the image, lens and object plane intersect in one point, so that sections of the eye appear with large depth-of-focus. Scheimpflug images suffer from geometrical distortion (due to tilt of the object, lens and image planes), and optical distortion (due to the fact that the different surfaces are viewed through anterior refracting surfaces). Ray-tracing techniques are therefore required to obtain more reliable crystalline surface geometry (Dubbelman & van der Heijde, 2001, Lapuerta & Schein, 1995). Scheimpflug research instruments (Brown, 1973, Dubbelman & van der Heijde, 2001, Koretz, Cook & Kaufman, 1997) have been used to study the shape of the crystalline lens and how it changes with accommodation (as shown in Chapter 4) or aging (Dubbelman & van der Heijde, 2001, Dubbelman, van der Heijde & Weeber, 2005). In the clinical literature, there are numerous reports of intraocular lens tilt and decentration measurements either longitudinally or comparing different types of lenses using commercial Scheimpflug instruments reports (Baumeister, Neidhardt, Strobel & Kohlen, 2005, Hayashi, Hayashi, Nakao & Hayashi, 1998, Jung, Chung & Baek, 2000, Kim & Shyn, 2001, Nejima, Miyata Honbou, Tokunaga, Tanabe, Sato & Oshika, 2004, Sasaki, Sakamoto, Shibata, Nakaizumi & Emori, 1989, Meng-Chi, Lin-Ghung, Chao-Yu & Han-Chin., 1998). In these instruments the optical distortion is presumably not corrected. Only a recent study of IOL tilt and decentration in eyes with phakic lenses (Coopens, Van den Berg & Budo, 2005), using a Nidek Scheimpflug system, mentions that images were corrected using custom algorithms.

The availability of new Scheimpflug commercial instruments may make the measurement of IOL tilt and decentration more accessible. However, powerful data

processing routines, a careful assessment of the limitations of the technique, and experimental validations are necessary before this information can be used reliably.

In this chapter we present measurements of IOL tilt and decentration of intraocular measurements in a water cell model eye and in patients, using a custom-built Purkinje imaging system and a Pentacam Scheimpflug imaging with custom algorithms. To our knowledge, this represents the first assessment of the accuracy of the techniques to measure IOL tilt and decentration, and the first cross-validation of Scheimpflug and Purkinje imaging to measure tilt and decentration.

2. METHODS

2.1 Purkinje imaging

A system for phakometry and lens tilt and decentration measurements based on phakometry and implemented at the Instituto de Optica (CSIC) was used in the study. The optical set up, processing algorithms and validations have been described in the chapter 2 of this thesis. In brief, the system consists of 1) two illuminating channels (for measurements on right and left eyes) with collimated light from IR LEDs, at an angle of 12 deg, horizontally; 2) an imaging channel with an IR-enhanced CCD camera provided with a telecentric lens mounted in front of the eye and conjugate with the eye's pupil; 3) a fixation channel with a minidisplay, a collimating lens and a Badal system, which allows projection of visual stimuli both foveally and at different eccentricities, as well as correction of refraction. The system sits on a 500 × 400 mm optical table. Software written in Visual Basic (Microsoft Visual Studio 6.0, Redmond, WA) controls automatically the image acquisition, LED switching and stimulus display. Data processing is performed using Matlab (Mathworks Inc., Natick, MA) and the optical design program Zemax (Focus Software, Tucson, AZ). The detection of Purkinje images PI, PII and PIII and pupil center in the pupillary images is performed using Gaussian fitting with routines written in Matlab. The processing routines assume that P1, P3 and P4 (positions of PI, PII and PIII relative to the center of the pupil) are linearly related with eye rotation (β), lens tilt (α) and lens decentration (d).

$$P1 = E \beta$$

$$P3 = F \beta + A \alpha + C d$$

$$P4 = G \beta + B \alpha + D d,$$

These equations are applied to both horizontal and vertical coordinates. Coefficients A-G are obtained using a computer model eye (simulated using biometric data available

for each eye). IOL decentration is referred to the pupil center. IOL tilt is referred to the pupillary axis.

2.2 Scheimpflug imaging

A commercial Scheimpflug imaging System (Pentacam, Oculus) was used to image sections of the anterior segment of the eye at different meridians (25), by projecting a slit (blue light). The software of the system corrects geometrical distortion but shows uncorrected images. Since we work directly on the images captured, a routine to correct this distortion was implemented (de Castro et al., 2007). The commercial software provides quantitative information of the anterior and posterior corneal surfaces, but not the crystalline lens/IOL. In addition, the edge detection routines of this software usually fail to detect the edges of certain types of IOLs (i.e. acrylic) due to their different scattering properties from the crystalline lens. We have developed algorithms that work directly on the raw images and calculate IOL tilt and decentration. These include:

- 1) Correction of the geometrical distortion of the images.
- 2) Routines to find the edges of cornea and intraocular lenses.
- 3) Routines fitting the edges of the pupil and the lens to find the pupil center, IOL center, IOL tilt, and eye rotation.
- 4) These procedures are applied to each of the 25 sections obtained at each meridian.
- 5) IOL decentration is obtained from the distance between the IOL center and the pupillary axis.

2.3 Physical model eye

A physical model eye was built by Alberto de Castro (de Castro et al., 2007) specifically for this study, where nominal values of IOL tilt and decentration can be set. Figure 5.1 shows a photograph (A) and a schematic diagram (B) of the model eye. It consists of a PMMA water cell model, with a PMMA contact lens simulating the cornea and IOL lenses on a XYZ micrometer stage and rotational stage. The cornea was built by a contact lens manufacturer (AR3 Vision, Madrid, Spain) with parameters similar to the Gullstrand eye model (corneal diameter: 11.20 mm, anterior corneal radius: 7.80 mm, posterior corneal radius: 6.48 mm, central thickness: 500 μm). Different intraocular lenses with spherical or aspheric designs from different manufacturers (Pharmacia, Alcon and A.M.O.) with IOL powers of 19, 22 and 26 D were used in place

of the crystalline lens. Decentration was achieved in the horizontal direction, with a precision of 0.1 mm. Tilt of the IOL was achieved in the horizontal direction, with a precision of 0.01 degrees. The anterior chamber depth could be varied, but for the purpose of this study we kept it constant at 5 mm.

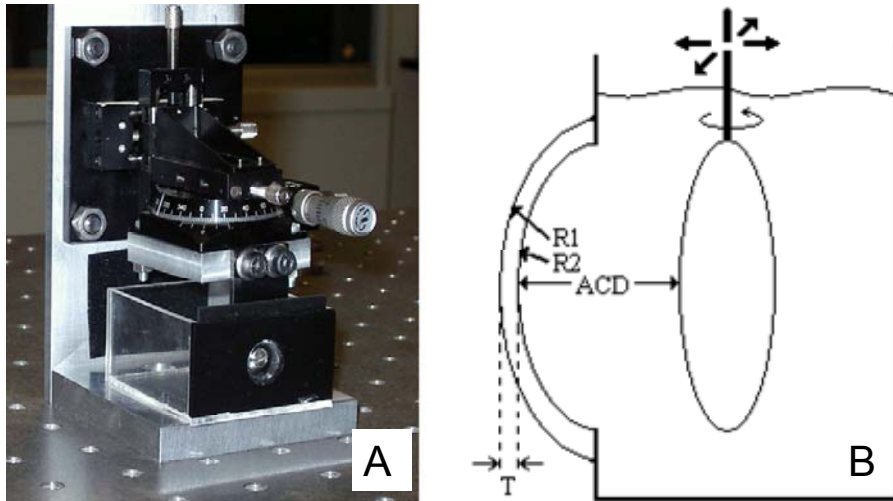


Figure 5.1. A. Photograph and B. schematic diagram of the physical model eye developed for this study. A PMMA contact lens simulates the cornea ($R1= 7.80$ mm, $R2= 6.48$ mm, $T= 500$ mm). IOLs are positioned with an XYZ micrometer stage and rotational stage.

2.4 Patients

For this study 21 eyes from 12 patients (average age 72 ± 8 years) with intraocular lenses implanted were measured. Time after surgery was at least six months. IOLs had aspherical designs. All protocols adhered to the declaration of Helsinki and followed protocols approved by Institutional Review Boards. All patients signed informed consents after receiving an explanation of the purposes of the study.

2.5 Experimental protocols

The artificial eye is fixated in a translational XYZ and then aligned with the system. The main difference with respect to measurements on patients is that the optical axis of the model eye is collinear with the optical axis of the instrument (as opposed to the line of sight).

Measurements were done for horizontal decentrations ranging from 0 to 2 mm (every 1 mm) and horizontal tilts (around the vertical axis) ranging from 0 to 4 degrees (every

1 deg). Since the IOL does not rotate around its own axis, induced decentration was compensated for the tilted conditions. Alternate measurements with both the Purkinje and Scheimpflug systems were made for each condition of tilt and decentration.

Measurements on patients were performed under pupil dilatation with tropicamide 1%. In the Purkinje apparatus, subjects were aligned with respect to the line of sight while they viewed foveally a fixation target presented in the minidisplay. Stabilization was achieved with a dental impression. Series of images were captured for different fixation angles (with fixation stimuli presented from -3.5 to 3.5 deg horizontally and from -2.5 to 2.5 deg vertically). Although only a snapshot is necessary to obtain IOL tilt and decentration, different eccentricities were tested to avoid overlapping of the Purkinje images. To assess the measurement reproducibility the whole procedure was repeated 3 times. For Scheimpflug imaging the subject fixates foveally a fixation target. Three series of 25 images were obtained per eye.

Data processing of Purkinje imaging data requires several individual ocular biometry data to obtain coefficients A-G in the Phillips equations. For the artificial eye these were taken from nominal values. In patients we measured anterior corneal radius and anterior chamber depth from optical biometry (IOLmaster, Zeiss). The radii of curvature of the anterior and posterior IOL surfaces were measured using the phakometry mode of our Purkinje imaging system (see (Rosales & Marcos, 2006)) if the geometry of the lens was not known.

3. RESULTS

3.1 Purkinje imaging and Scheimpflug raw data

Figure 5.2 shows typical images for the artificial eye captured with the Purkinje imaging system (top) and the Scheimpflug camera (bottom) respectively. Left images correspond to an eye with a 2-mm decentered silicone IOL, and right images to an eye with a 3-deg tilted acrylic IOL. Nominal decentration and tilt were set with the micrometer stages in the artificial eye. Purkinje images PI, PIII and PIV have been marked on Figure 5.2, and the detected edges and fitting circumferences are superimposed on the Scheimpflug sections of Figure 5.2. Figure 5.3 shows typical examples of Purkinje (left) and Scheimpflug (right) images for one real eye. Differences in the diffusing properties of the real cornea and PMMA cornea of the artificial eye can be observed.

The relative positions of PI, PIII and PIV with respect to the center of the pupil are detected from images like those shown in Figure 5.2 and 5.3, and data are processed as explained above to obtain Purkinje tilt and decentrations. The centers of curvature of the corneal and lens surfaces and pupil center are computed from each of the 25 Scheimpflug sections as those shown in Figure 5.2 and 5.3.

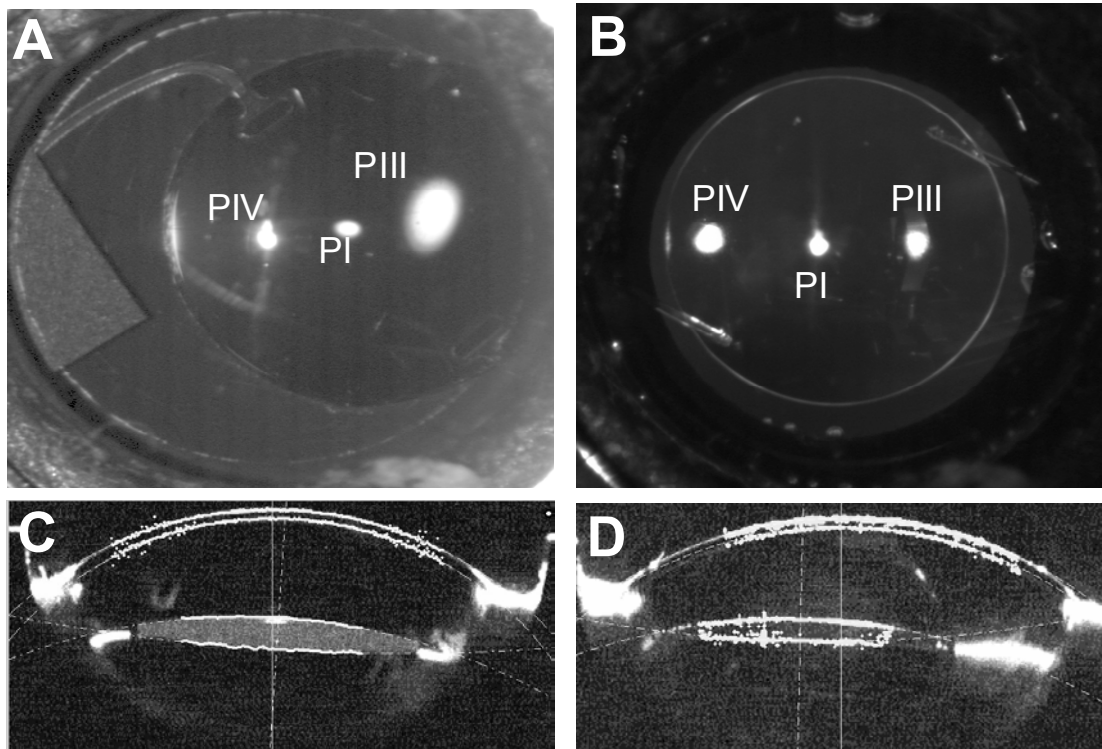


Figure 5.2. **A. B.** Raw images obtained using the Purkinje imaging system and Scheimpflug system **C. D** from the model eye. The examples correspond to a tilted silicone IOL (**A, C**) and a decentered acrylic IOL (**B, D**). PI, PIII and PIV are marked on the image from the Purkinje system. The fitted curves and calculated axes have been superimposed on the Scheimpflug image.

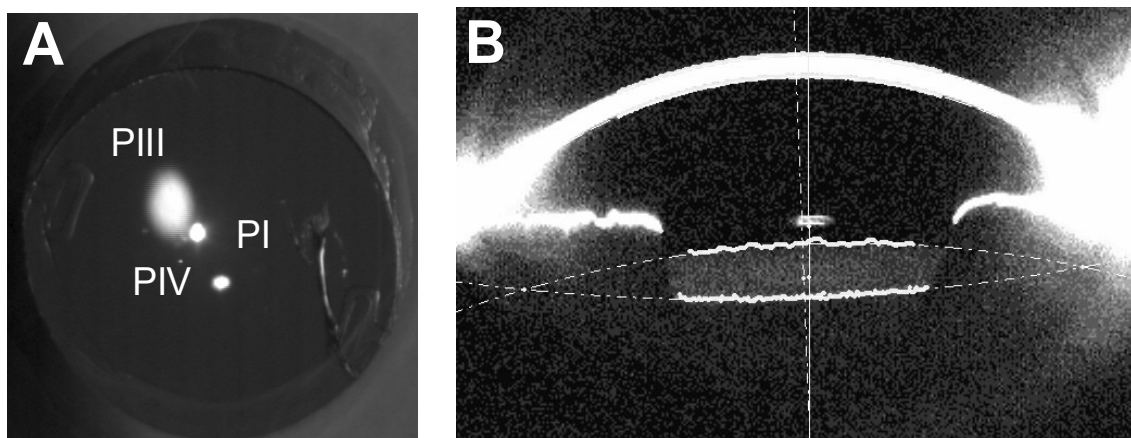


Figure 5.3. Raw images from the Purkinje (**A**) and Scheimpflug (**B**) systems in a real eye. As in Figure 2, the Purkinje images locations and fitted curves and calculated axis have been superimposed.

3.2 IOL tilt and decentration in the physical model eye

Figure 5.4.A shows measured tilt from Purkinje imaging, and 5.4.B measured tilt from Scheimpflug imaging as a function of nominal tilt in the artificial eye, for three different IOLs. The solid line represents the ideal results. There is a good correspondence between nominal and measured values for both Purkinje imaging (average slope= 1.088, average absolute discrepancy= 0.279 deg) and Scheimpflug imaging (average slope= 0.902 average absolute discrepancy= 0.243 deg). Error bars represent the standard deviation of repeated measurements. Figure 5.4.C shows measured decentration from Purkinje imaging, and 4.D measured decentration from Scheimpflug imaging as a function of nominal decentration in the artificial eye, for three different IOLs. There is a good correspondence between nominal and measured values for Purkinje imaging (average slope = 0.961, average absolute discrepancy = 0.094 mm and a higher disagreement for Scheimpflug imaging (average slope= 1.216, average absolute discrepancy= 0.228 mm), where there is a consistent overestimation for two of the measured lenses.

3.3 IOL tilt and decentration in patients' eyes

Figure 5.5 shows tilt (A & B) and decentration (C & D) of intraocular lenses for right eyes (A & C) and left eyes (B& D) of real patients. Results from Purkinje imaging are shown as open symbols and from Scheimpflug imaging as solid symbols. Positive tilts around X-axis indicate that the superior edge of the lens is moved forward and viceversa for negative tilts around X-axis. Positive tilts around Y-axis stand for nasal tilt and indicate that the nasal edge of the lens is moved backwards) and viceversa for a negative tilt around Y-axis, in right eyes. A positive tilt around Y-axis stands for temporal tilt (nasal edge of the lens moves forward) in left eyes. A positive horizontal decentration stands for a nasal decentration in right eyes and temporal in left eyes. Positive vertical decentration (d_y) indicates that the lens is shifted upwards and vice versa for negative. There is clear mirror symmetry in tilt (as measured with both techniques) and less systematic trend for decentration in this group of eyes.

We found average absolute tilts around X of 1.89 ± 1.00 deg (Purkinje) and 1.17 ± 0.75 deg (Scheimpflug), average absolute tilts around Y of 2.34 ± 0.97 deg (Purkinje) and 1.56 ± 0.82 deg (Scheimpflug), and average absolute horizontal decentration of 0.34 ± 0.19 mm (Purkinje) and 0.23 ± 0.19 mm (Scheimpflug), and average absolute

vertical decentration of 0.17 ± 0.23 mm (Purkinje) and 0.19 ± 0.20 mm (Scheimpflug). Figure 5.6 compares tilts and decentrations measured with Scheimpflug and Purkinje imaging. The results with both techniques are highly significantly ($p < 0.001$) correlated for horizontal decentration ($r = 0.764$) and tilt around Y axis ($r = 0.762$), i.e. horizontal displacements of the lens. For vertical decentrations and tilts around X, the correlations are not significant, and the estimated values are close to the measurement error and method accuracy.

Repeatability of both the Purkinje and Scheimpflug methods were found to be high: mean average standard deviation of repeated measurements were 0.61 and 0.20 degrees for tilt and 0.05 and 0.09 mm for decentration, for Purkinje and Scheimpflug respectively. An ANOVA for repeated measures was used to test whether the mean value (for each type of measurement) is representative of data. We found this to be the case in all conditions.

After this analysis, intraclass correlation coefficients were calculated to assess the reliability of the methods (since the intraclass is sensitive both to random error and to systematic bias). We found that the methods were reliable for tilt around Y (intraclass coefficient = 0.830) and for decentration in X (intraclass coefficient = 0.836).

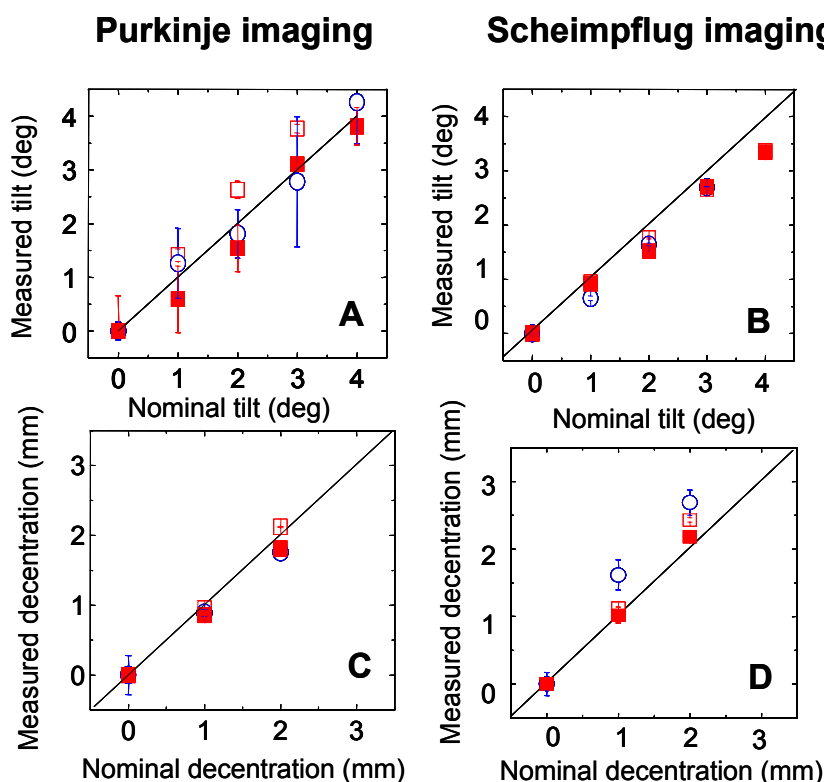


Figure 5.4. Experimental IOL tilt (A, B) and decentration (C, D) for the model eye for three different lenses (plotted with different symbols) as a function of nominal values of tilt and decentration using Purkinje imaging (A, C) and Scheimpflug imaging (B, D). Nominal tilt ranged from 0 to 4 degrees and nominal decentration ranged from 0 to 2 mm. The ideal X=Y line has also been plotted.

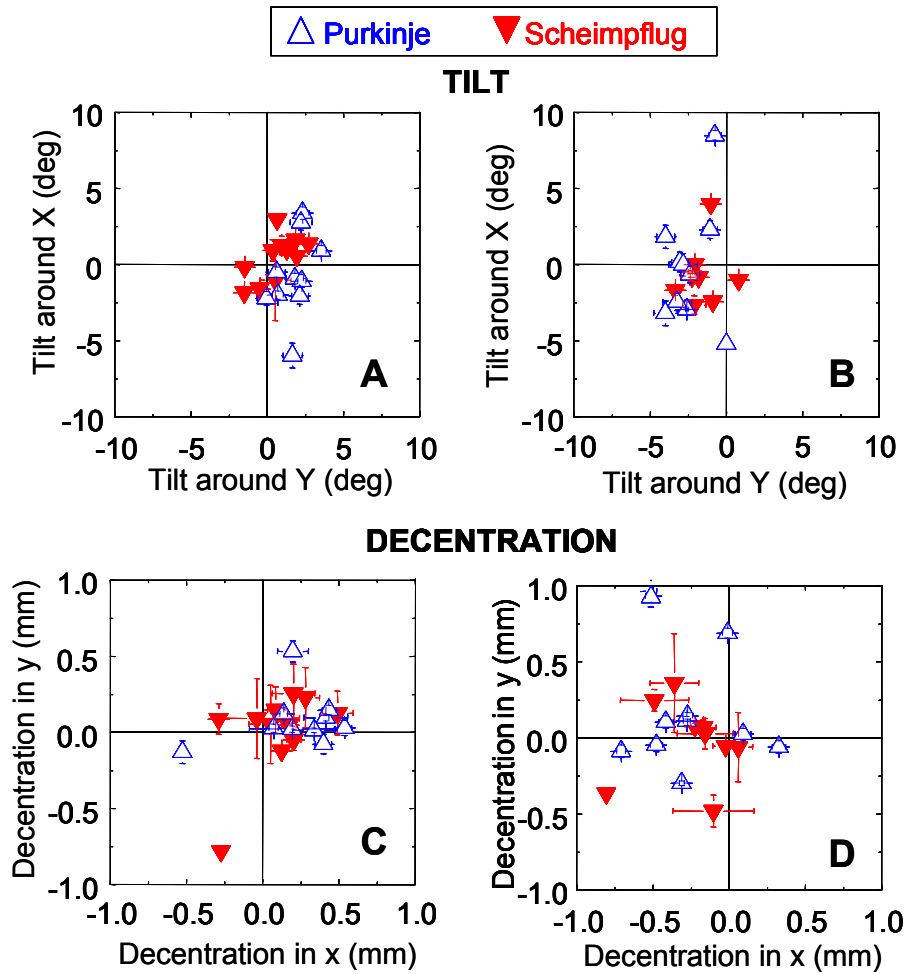


Figure 5.5. Tilt (**A**, **B**) and decentration (**C**, **D**) for right and left eyes of patients, using Purkinje (open symbols) and Scheimpflug (solid symbols) imaging. Refer to the text for details on sign conventions. The sign of the tilt around x-axis has been changed to allow a more graphical representation of lens positioning, assuming a frontal view of the patients' eyes. Both techniques show a forward (toward the cornea) tilt of the nasal side of the IOL, and a clear mirror horizontal symmetry of tilt across right and left eyes. Also, both techniques show a nasal displacement of the IOLs, and a clear mirror horizontal symmetry of tilt across right and left eyes.

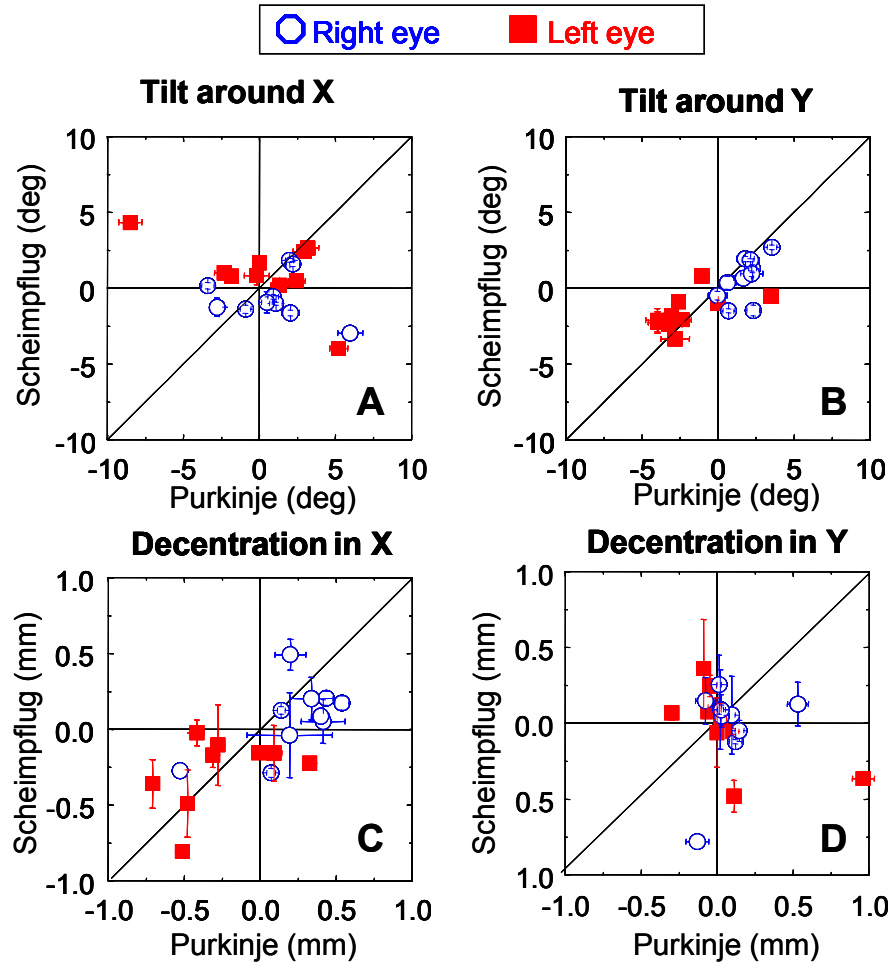


Figure 5.6. Comparison of the horizontal and vertical components of IOL tilt and decentration between Scheimpflug and Purkinje techniques. The ideal X=Y line is also shown. The correlations are statistically significant ($p < 0.001$) for the tilt around x-axis and horizontal decentration.

4. DISCUSSION.

4.1 Limitations of the techniques

The Purkinje imaging system has been extensively validated computationally and experimentally in previous studies (Rosales, Dubbelman, Marcos & Van der Heijde, 2006), as has been shown in Chapters 2 and 3 of this thesis. Computer simulations using eye models and the actual optical configuration of the system show that deviations from spherical model eyes due to corneal asphericity or corneal irregularities and anterior and posterior lens surfaces asphericities did not affect significantly the results of lens tilt and decentration.

Scheimpflug images from the Pentacam system are not corrected from optical distortion, and the CCD images also suffer from geometrical distortion. The former is corrected by software at the corneal level, but not at the crystalline or IOL lens level. The second can be compensated using calibration grids. This is implemented in the commercial software to provide corrected biometry values, and a routine to compensate the raw images has been developed.

Our measurements with both techniques show a high reproducibility. The Purkinje imaging system has some limitations when lenses are very flat, for which PIII is quite large. The system also relies on the appropriate measurement of the anterior and posterior lens radii of curvature. Scheimpflug imaging requires sufficient pupil dilation to visualize the posterior lens surface and collaboration from the patients to fixate for 1.5 seconds without moving while illuminated with a blue light (as opposed to IR illumination and 30 exposure times in the Purkinje imaging system). Scheimpflug imaging also poses some challenges with low diffusing IOLs. Optical and geometrical distortion of the Scheimpflug images (as obtained directly from the CCD) produce slight discrepancies of the measured tilt and decentration, which improve with the correction of the geometrical distortion.

In real eyes, both techniques agree well, in general, for the horizontal IOL tilt and decentrations. The larger discrepancies, particularly for vertical decentration may be attributed to the proximity of the decentration measurements to the nominal accuracy of the techniques.

4.2 Comparisons to previous studies and implications

In this study we present an experimental validation of the Purkinje imaging system developed in this thesis to measure tilt and decentration of IOLs using a physical model eye. We also proposed a new robust method to calculate tilt and decentration of an IOL using a commercial Scheimpflug imaging system, which is validated using the same physical model eye. A comparison of tilt and decentration measurements in real eyes using both techniques is also presented.

Purkinje and Scheimpflug methods have been used before to measure tilt and decentration of IOLs. To our knowledge, only the reports of Barry (Barry, Dunne & Kirschkamp, 2001) and Rosales (Rosales & Marcos, 2006) were based on thoroughly validated Purkinje imaging methods. Several studies report tilt and decentration measured with Scheimpflug imaging, in most cases from two sections of the anterior

segment captured at perpendicular meridians. Coopens et al (Coopens et al., 2005), working with a modified Nidek system, used two or more images to create a redundant data set to check the procedure. In the present study we used combined information from 25 meridians. To our knowledge, only Coopens et al. corrected the Scheimpflug images from geometrical and optical distortion to measure tilt and decentration of intraocular lenses. We have found that not correcting for geometrical distortion cause slight discrepancies in the measured values.

Our results (mean values with Scheimpflug and Purkinje in this study are decentrations of 0.21 ± 0.28 mm horizontally and 0.03 ± 0.38 mm vertically and tilts of -0.26 ± 2.63 deg around x-axis and 1.54 ± 1.50 around y-axis. Decentrations in X and tilts around Y being nasal for both eyes. In general, the amounts of tilt and decentration that we report are lower than the earliest reports in the literature. For example, Philips (Phillips, Perez-Emmanuelli, Rosskothén & Koester, 1988) reported average decentrations of 0.7 ± 0.3 mm and tilts of 7.3 ± 3.0 deg without specifying direction of tilt or decentration. One report of IOL position after transcleral implantation show systematically high amounts of tilt and decentration (an average IOL tilt of 5.97 ± 3.68 deg and average decentrations of 0.63 ± 0.43 mm), which the authors attribute to the implantation technique (Ismet, 2000). Our results are more comparable with those from more recent studies, reporting lower values of tilt and decentration, and are probably associated with an improvement of the surgical procedure. These results are close to the pilot data of IOL tilt and decentration presented in Chapter 2 (Rosales & Marcos, 2006): 0.87 ± 2.16 deg for tilt around X-axis, 2.3 ± 2.33 deg for tilt around Y-axis, and 0.25 ± 0.28 mm for horizontal decentration and -0.41 ± 0.39 mm for vertical decentration.

Other studies using non-corrected Scheimpflug images reported average tilts between 2.61 ± 0.84 deg (three-piece acrylic IOLs, (Meng-Chi, Lin-Chung, Chao-Yu & Han-Chin, 1998) and 3.4 ± 2.02 deg (silicone IOLs, (Kim & Shyn, 2001)) and average decentrations of 0.29 ± 0.26 mm to 0.37 ± 0.19 (Meng-Chi et al., 1998). To our knowledge only one study mentions interocular mirror symmetry for tilt and decentration, with phakic IOLs (Coopens et al., 2005). While most studies and techniques provide similar average values, which agree well with the average values reported here using both Purkinje and Scheimpflug, we have shown that in individual patients some discrepancies across techniques may be found. This is particularly important when using Scheimpflug images that have not been corrected for geometrical and optical

distortion, as are the raw images provided by commercially available instruments such as the Pentacam.

Finally, the amounts of tilt and decentration found in patients are in general low, and particularly for the decentration are of the order of the resolution of the techniques in many patients. The clinical relevance of tilts and decentrations of these amounts is likely limited (Rosales & Marcos, 2007) although there are case reports in the literature where they result in decreased visual function (Oshika, Kawana, Hiraoka, Kaji & Kiuchi, 2005). The impact of IOL tilt and decentration on optical aberrations of pseudophakic eyes will be addressed in Chapter 8.